ELEKTROMECHANIKUS SEBESSÉGVÁLTÓ AKTUÁTOR DINAMIKAI MODELLEZÉSE

DYNAMIC MODELING OF AN ELECTROMECHANICAL GEARSHIFT ACTUATOR

Ayham Aljawabrah, PhD Student, aaljawabrah@edu.bme.hu
Dr. László Lovas, associate professor, lovas.laszlo@kjk.bme.hu
BME Department of Railway Vehicles and Vehicle System Analysis

ABSTRACT
The gearshift mechanism is an essential part of the automated shift control system. Among the available types, the electromechanical gearshift mechanism is more reliable. This paper aims to analyze an electromechanical gearshift mechanism used in a sequential transmission. Analyse and modeling of the system dynamics show that the resulting system is highly nonlinear. Simulated tests are performed in the system model at different input voltages to study the open loop system response and its nonlinear behavior.

1 INTRODUCTION

In motor vehicles, the gearbox contains different gear ratios, as it is used to set the driving torque to fit the different driving conditions. It provides the required high torque for starting the vehicle. After the start, the required torque decreases, so the gearbox will provide the optimum torque to the wheel at given speed. During the operation, the selected transmission ratio is influenced by the actual vehicle driving conditions. Thus, it is either determined by the driver of the vehicle, via the gear selector in the passenger cabin, as in a conventional manual transmission (MT), or by a transmission control unit (TCU), as in stepped automatic transmissions (AT). A MT has higher efficiency compared to the conventional ATs. However, ATs have complete control over gear selection, based on factors such as driver demand, speed, and road gradient. Here the TCU chooses the appropriate gear ratio, so this ensures the ICE operating in its most efficient speed range for a given vehicle load [1].

In an attempt to combine the benefits of MTs and ATs, automated manual transmissions (AMT) and dual clutch transmissions (DCT) have been developed. However, DCTs are more expensive than AMTs as their technology is in an early stage, and they have a longer time-to-market due to the extra development required to design the transmission components and implement the control system of the transmission [2].

Automated Mechanical Transmission (AMT) is a modified version of traditional MT. Specifically, Automated Shift Control System (ASCS) is added to AMT based on mechanical transmission to achieve automatic shift operation of vehicles. ASCS usually has three main parts: sensors, transmission control unit and executive mechanism. A crucial part of ASCS is an executive mechanism of high accuracy and reliability, which, in the meanwhile, is the key technology for realizing automatic control of AMT of vehicles [3]. The actuation mechanism can be pure hydraulic, electrohydraulic, electropnuematic, or electromechanical. As compared with others, the electromechanical shift mechanism has the advantage of compact structure, small size, easy operation, reliability, and energy saving abilities [4]. Electromechanical actuators are widely used in vehicle transmissions [4-6].

The electromechanical actuators usually include an AC servo motor and a cam mechanism, and system dynamics usually is nonlinear. However, the actuator shall have an accurate dynamic response to the TCU.

In this paper, an electromechanical gearshift mechanism used in a sequential transmission is analyzed. The system dynamics are modeled. Then, the system model is simulated with Simulink to study the open loop system response and the states trajectories.

2 GEARSHIFT ACTUATOR

2.1 Actuator geometry

The gearshift mechanism under consideration (Figure 1) is a part of a 4 speed sequential transmission. It consists of an electric motor (EM), a disk-type cam roller-follower mechanism, and two shifting forks. The EM is a *24V* servo AC motor, which provides the rotational motion for the disk, while the cam follower mechanism converts the rotational motion to a linear one. The disk has two slots for forks 1 and 2 respectively, and the slots profiles govern the coupled rotational-linear motion. The forks can move linearly only. One fork is attached to the 1st and 2nd gears (Fork 1) and the other to the 3rd and 4th gears (Fork 2).

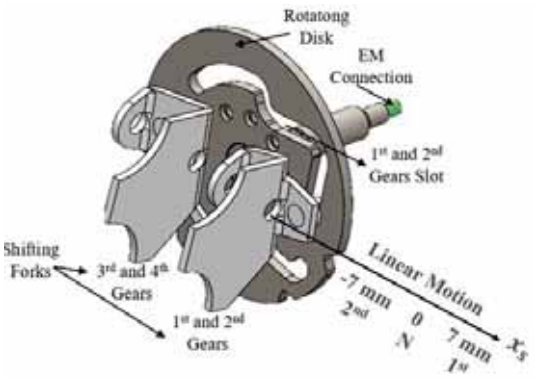

Figure 1 Shifting Mechanism Geometry

The linear position x_s of the forks as a function of the disk angle θ_k is shown in Figure 2, while the disk's angular position and the forks' linear position are summarized in Table 1.

Table 1 Disk angle and fork positions for different gear ratios

Gear	1st	2nd	3rd	4th
θ_k *(deg)*	34	70	108	144
	Fork 1 / Fork 2	Fork 1 / Fork 2	Fork 1 / Fork2	Fork 1 / Fork 2
x_s *(mm)*	7 / 0	-7 / 0	0 / 7	0 / -7

2.2 Dynamic modeling

The focus of this paper is on 1st and 2nd gears, so, the disk angle range considered is in the interval [*0, 90*] *deg*. The 1st and 2nd gears slot profile consist of eleven straight lines and circular arc segments. The linear displacement will be a piecewise function of the disk (or electric motor) rotation angle (θ_k).

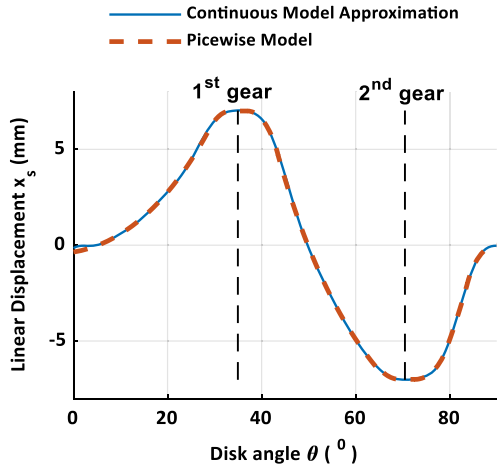

Figure 2 Linear Displacement x_s

For simplicity, the piecewise profile has been approximated by an eight terms Fourier series, as Eq. (1) shows. Figure 2 shows the comparison between the piecewise model and Fourier series approximation, and the goodness of the fitting R^2 is 0.9999. At neutral gear, the sliding sleeve is at *0 mm*, then it moves to *7 mm* to engage the first gear, then it moves back to *-7 mm* to engage the second gear.

$$x_s = a_0 + \sum_1^8 (a_k \cos(k\omega\theta_k) + b_k \sin(k\omega\theta_k)) \quad (1)$$

From Eq.(1), Eq.(2), and Eq.(3) can be obtained.

$$\dot{x}_s = \frac{dx_s}{d\theta_k}\dot{\theta}_k \quad (2)$$

$$\ddot{x}_s = \frac{d^2x_s}{d\theta_k^2}\dot{\theta}_k^{\,2} + \frac{dx_s}{d\theta_k}\ddot{\theta}_k \quad (3)$$

The linear force equilibrium is given according to Eq.(4):

$$m\ddot{x}_s = F \quad (4)$$

$$F = F_{act} - F_x \quad (5)$$

The force F_x includes the internal friction forces between the follower and the cam as well as the sliding friction forces. The sliding friction forces include the Coulomb friction force and the viscous friction. However, two model simplifications are considered

- The internal friction forces are ignored since the mechanism has a roller follower.
- The sliding friction forces are not considered since the model is highly nonlinear and the response of the system itself is on focus.

Based on this, F_x is neglected.

A torque T results from the interactions with the cam-follower mechanism. Based on the law of conservation of energy, the relation between the interface force F_{act} and the torque T can be written according to Eq.(6). Then, Eq. (3), Eq.(4), Eq.(5), and Eq.(6) are combined to obtain a relation for the torque T as shown in Eq.(7):

$$T = F_{act}\frac{dx_s}{d\theta_k} \quad (6)$$

$$T = m\left(\frac{dx_s}{d\theta_k}\right)^2\ddot{\theta}_k + m\frac{dx_s}{d\theta_k}\frac{d^2x_s}{d\theta_k^2}\dot{\theta}_k^{\,2} \quad (7)$$

The torque equilibrium on the output shaft of the electric motor is given according to Eq.(8). Eq.(9) results by substituting Eq.(7) into Eq.(8), and it represents the coupled linear-rotational dynamics for the cam-follower mechanism.

$$J_k\ddot{\theta}_k = T_L - T \quad (8)$$

$$\left(m\left(\frac{dx_s}{d\theta_k}\right)^2 + J_k\right)\ddot{\theta}_k + m\frac{dx_s}{d\theta_k}\frac{d^2x_s}{d\theta_k^2}\dot{\theta}_k^{\,2} = T_L \quad (9)$$

Since Eq. (1) is nonlinear, Eq. (9) is nonlinear too. Here, m is the mass of the linearly moving parts, and J_k is the inertia of the disk. The load torque T_L is supplied by the electric motor. The electric motor dynamics are shown in Eq. (10) for the electrical part and Eq.(11) for the mechanical part. Here, K_t is the torque constant, K_e, back electromotive force constant, and R and L are the electrical resistance and inductance.

$$L\frac{di}{dt} + Ri = V - K_e\dot{\theta} \quad (10)$$

$$J_M\ddot{\theta}_k = K_t i - T_L \quad (11)$$

Eq.(9) and (11) can be combined to form Eq.(12):

$$\left(m\left(\frac{dx_s}{d\theta_k}\right)^2 + J_k + J_M\right)\ddot{\theta}_k + m\frac{dx_s}{d\theta_k}\frac{d^2x_s}{d{\theta_k}^2}{\dot{\theta}_k}^2 = K_t i \quad (12)$$

The equivalent inertia is shown in Eq. (13). It is obvious that the system has time-dependent inertia, which is a consequence of the nonlinear relationship between the linear and rational motion

$$J_{eq} = m\left(\frac{dx_s}{d\theta_k}\right)^2 + J_k + J_M \quad (13)$$

3 RESULTS

The model parameters are listed in Table 2. Figure 3 shows the change in the time-varying inertia J_{eq} and the first derivative $dx_s/d\theta_k$, with respect to the disk angle θ_k.

Table 2 System parameters

J_M	720×10^{-9} kg.m^2	J_k	224.43×10^{-6} kg.m^2
K_e	0.191 V.s/rad	K_t	0.1125 N.m/A
L	3.2×10^{-3}H	R	0.9 Ω
m	0.6 kg		

Before the 4.2^o disk angle, there is no change in the inertia since there is a small change in the axial displacement x_s and it is clear from $dx_s/d\theta_k$ curve. However, x_s changes beyond this angle and the inertia increases to 5.2×10^{-4} kg.m^2 at 30^o, then decreases suddenly at 32^o and reaches 2.25×10^{-4} kg.m^2 at 34^o when Fork 1 approaches its final position for the 1st gear, where $dx_s/d\theta_k$ is zero.

Then the inertia does not change until 37^o when it suddenly increases until it reaches a maximum of 14.4×10^{-4} kg.m^2 at 44^o, where the maximum $dx_s/d\theta_k$ is located. Afterwards, the inertia decreases until it reaches 2.25×10^{-4} kg.m^2 at 70^o, where the 2nd gear is engaged.

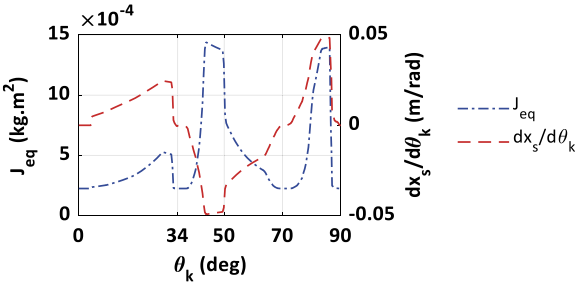

Figure 3 Time-varying inertia

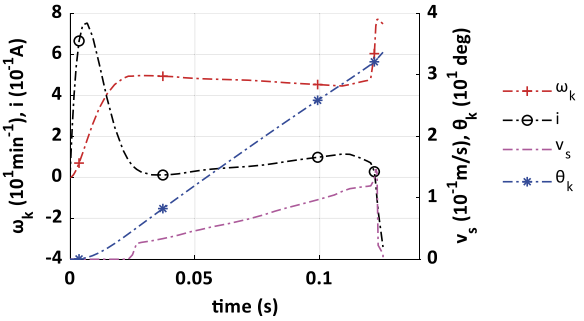

Figure 4 Open loop response N-1st gearshift at 1V input

The shifting mechanism has been simulated with Simulink with constant input voltage to study its nonlinear behavior, and Figure 4 shows the system's open-loop response for *1V* input. In Figure 4, the motor angular velocity and current increase until time *0.007s* but the current start to decrease from 0.*75A* when the back electromotive force (EMF) is high. The angular velocity reaches $50min^{-1}$ and then starts to decrease at *0.023s* when θ_k is 4.2^o, where J_{eq} starts to increase as shown in Figure 3. At *0.023s*, the motor starts to feel more inertia and according to the law of energy conservation, the velocity shall decrease, which preserves the system's available energy. In the period [*0.037, 0.11*] *s* the system shows a linear response for the current and angular velocity, where θ_k is in the period [*8, 26*] *deg*. This linear response is clearly seen in θ_k curve. At *0.12s*, θ_k is 31.5^o where J_{eq} decreases rapidly as seen in Figure 3, and this causes the angular velocity to increase rapidly, according to the energy conversation laws. On the other hand, the current decreases rapidly due to high EMF. Regarding the axial velocity, its value is zero before 4.2^o since the linear position does not change and $dx_s/d\theta_k$ is zero, even though there is a rotational motion. In fact, in the interval [*0, 4.2*] *deg,* the system is linear, where all nonlinear terms in Eq.(12) fall to zero, and the system's differential equation (DE) system describes a simple linear EM.

Figure 5 shows the system response for *5V* input, and the state variables show a similar trend to the ones for unit step voltage (Figure 4), but the current and angular velocity reach *3.8A* and

210min^{-1}, in the disk angle region [*0, 4.2*] *deg*, compared to *0.75A* and *50min^{-1}* in *1V* step input.

The system nonlinearity is clearer, especially in the period [*0.037, 0.11*] *s*, compared to the period [*0.037, 0.11*] *s* in Figure 4. In fact, the increased nonlinear terms effects is governed by the shifting time and the time constant τ for the linear part. The linearized model part is a simple EM DE, or RL circuits linear differential equation (LDE) system, and all besides the mechanical side LDE. The time constant τ for RL circuit is *L/R* or *3.56 ms* and it is well-known that a linear system needs 4τ to reach *98%* of its steady state after a step input is supplied to it. In the case of *1V* input, the change in J_{eq} is slower than the *5V* case, and the system has more time to retain its new steady state, due to the change in J_{eq}.

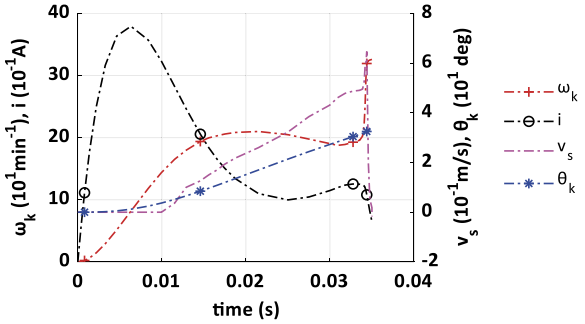

Figure 5 Open loop response N-1st gearshift at 5V input

Figure 6 shows the system response for 1st to 2nd gearshift under *5V* step input. For 1st to 2nd, the system makes *14mm* displacement compared to *7mm* in the case of N-1st gearshift, so that, the 1st to 2nd has *0.043s* shift time compared to *0.035s* in N-1st case, even though both have same input voltage. In the disk angle region [*34, 37.7*] *deg*, the system does not have linear motion which is clear from the v_s curve, and the system behaves linearly in this region. The current peak inside this region is *3.8A* which is identical to that seen in Figure 5, which is a clear clue that the nonlinear terms have no effect when there is no linear motion. However, in Figure 5, the angular velocity is *210min^{-1}* at the end of this region compared to *150min^{-1}* in Figure 6, because in Figure 5, the system has *4.2^o* gap compared to *3.7^o* in Figure 6, before the linear motion starts. This grants the system more time to increase its speed before the linear motion starts.

4 CONCLUSION

In this work, the electromechanical gearshift mechanism dynamics were analyzed. Even though the considered gearbox has four gear ratios, the focus was on the *N-2nd* region. The coupled rotational-linear motion relation is nonlinear and based on that the system dynamics are modeled and the resulting model is nonlinear. The system input is identified to be the voltage *V* while its output is the disk angle. The model is simulated for N-1st and 1st -2nd shifting cases at *1V* and *5V* inputs, and the state variable trajectories were analyzed.

This work helps to find a linearized version of the equation system that can describe the reality with accurate precision, and is reliable enough to rely on for control design.

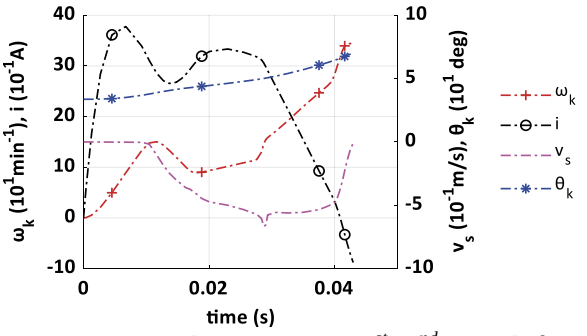

Figure 6 Open loop response 1st -2nd gearshift at 1V input

5 REFERENCES

[1] F. Rudolph, M. Schaefer, A. Damm, F. Metzner, I. Steinberg, The innovative seven speed dual clutch gearbox for Volkswagen's compact cars; Das innovative 7-Gang-Doppelkupplungsgetriebe fuer die Kompaktklasse von Volkswagen, (2007).

[2] A. Turner, K. Ramsay, R. Clark, D. Howe, Direct-drive rotary-linear electromechanical actuation system for control of gearshifts in automated transmissions, 2007 IEEE Vehicle Power and Propulsion Conference, IEEE, 2007, pp. 267-272.

[3] M. Jian-min, X. Jun-qiang, C. Hui-yan, Automated shift mechanism applied to AMT system of positive independent mechanical split path transmission, 北京理工大学学报自然版 (2) (2009) 108-112.

[4] J.L. Tao, H. Jin, W.S. Yuan, H.Y. Chen, Design on the Electromechanical Shift Mechanism of AMT, Applied Mechanics and Materials, Trans Tech Publ, 2011, pp. 355-359.

[5] B. Supriyo, S. Ariyono, B. Tjahjono, B. Sumiyarso, Electro-mechanical Transmission Ratio Shifter of Rubber Belt Continuously Variable Transmission for Motorcycle Applications, Journal of Physics: Conference Series, IOP Publishing, 2019, p. 012071.

[6] F. Zainuri, D.A. Sumarsono, M. Adhitya, R. Siregar, Design of synchromesh mechanism to optimization manual transmission's electric vehicle, AIP conference proceedings, AIP Publishing LLC, 2017, p. 020031.